Histopathology 2004, **45**, 119–124

The spectrum of pathological changes in severe acute respiratory syndrome (SARS)

O Y Cheung, J W M Chan,[1] C K Ng[1] & C K Koo[2]
Departments of Pathology and [1]Medicine and [2]Intensive Care Unit, Queen Elizabeth Hospital, Hong Kong

Date of submission 15 July 2003
Accepted for publication 24 September 2003

Cheung O Y, Chan J W M, Ng C K & Koo C K
(2004) *Histopathology* **45**, 119–124

The spectrum of pathological changes in severe acute respiratory syndrome (SARS)

Aims: To analyse the lung pathology of severe acute respiratory syndrome (SARS) and correlate the findings with the time sequence of the disease.
Methods and results: Ten patients with a clinical diagnosis of SARS, and virological confirmation of SARS coronavirus infection were identified. Histology in most cases showed diffuse alveolar damage, from early to late phases, and the changes corresponded to the time sequence. Other variable features include multinucleated giant cells, pneumocytes with cytomegaly and variable amounts of inflammatory cells and foamy macrophages. One case showed superimposed bronchopneumonia. No viral inclusions were found. Coronavirus particles were identified in pneumocytes by electron microscopy.
Conclusions: The predominant pathological process of SARS is diffuse alveolar damage and, in patients who die from the disease, there is evidence of organization and fibrosis. There are apparently no histological features specific for this disease, and the aetiological diagnosis depends on virological and ultrastructural studies.

Keywords: coronavirus, diffuse alveolar damage, lung pathology, severe acute respiratory syndrome

Abbreviations: DAD, diffuse alveolar damage; SARS, severe acute respiratory syndrome

Introduction

In early 2003 there was a major outbreak of an atypical pneumonia/severe acute respiratory syndrome (SARS)—a disease caused by a novel coronavirus (SARS coronavirus) in many countries, such as China including Hong Kong SAR, Canada, Singapore and Vietnam.[1,2] There were 8422 reported cases and 916 deaths worldwide as of 7 August 2003, bringing the crude mortality rate to 11%.[3] It spreads by droplet transmission with inhalation and mucous membrane contact being routes of entry.[4] Although many reports on this disease have already appeared in the literature, there are few providing detailed descriptions of the lung pathology.[1,2,5–8] We report here the spectrum of changes in 10 cases, including the ultrastructural findings.

Address for correspondence: Dr Cheung Oi Yee, Department of Pathology, Queen Elizabeth Hospital, Gascoigne Road, Kowloon, Hong Kong. e-mail: oycheung@yahoo.com

Materials and methods

All the available biopsy and autopsy tissues from patients with SARS were retrieved from the records of the Department of Pathology, Queen Elizabeth Hospital, Hong Kong. The clinical diagnostic criteria for SARS were: radiological evidence of infiltrates consistent with pneumonia and fever of >38°C or a history of such at any time in the previous 2 days and at least two of the following: (i) history of chills in the past 2 days, (ii) cough or breathing difficulty, (iii) general malaise or myalgia, (iv) known history of exposure. The confirmatory tests consisted of the serological demonstration of at least a four-fold rise in SARS coronavirus antibody titre; and reverse transcription-polymerase chain reaction (RT-PCR) for SARS coronavirus RNA on nasopharyngeal aspirate, nasopharyngeal swab, throat swab, tracheal aspirate or lung tissue. A positive result for SARS coronavirus was required in at least one of the above tests to confirm the diagnosis.

Ten cases were identified, including paramortem needle lung biopsy from six patients, full autopsy on

one patient, autopsy limited to the lungs from two patients, and an open lung biopsy. Two cases have been included in previous reports (Table 1). The biopsy or autopsy tissues were fixed in formalin, and processed routinely into paraffin blocks. Besides haematoxylin and eosin, Gram, Grocott and Ziehl–Neelsen (ZN) stains were performed to look for concomitant bacterial, fungal or mycobacterial infection. Electron microscopic study was performed on five cases. Clinical information and microbiological study results were retrieved and chest X-ray findings were reviewed.

Results

CLINICAL AND RADIOLOGICAL FINDINGS

The patients were aged 31–78 years; seven were male and three female. Six were previously healthy. Four had pre-existing disease including hypertension (patient 1), ventricular septal defect (patient 2), nephrotic syndrome (patient 3) and ischaemic heart disease and hypercholesterolaemia (patient 9). The commonest presenting symptom was fever (10 patients), followed by myalgia (6 patients) and cough (5 patients). Other symptoms included malaise, dyspnoea, diarrhoea, chills, rigor and headache. The initial chest X-ray showed unilateral haziness or air space infiltrates in eight patients and bilateral pulmonary infiltrates in two. All 10 cases showed evidence of infection by SARS coronavirus (Table 1). Seven of eight cases studied serologically showed a four-fold or greater increase in serum titre for the antibody against SARS coronavirus. Eight of nine patients with clinical samples for analysis had a positive result with RT-PCR for SARS coronavirus. Five of seven lung tissue samples were RT-PCR positive. There was no evidence of other viral infections on serological study and culture. The nine patients with paramortem biopsy or autopsy had been treated with corticosteroid, ribivarin, antibiotics and mechanical ventilation with supplementary oxygen before lung tissue was sampled. The terminal chest X-ray showed bilateral generalized air space consolidation in all patients. The time from onset of symptom to death ranged from 8 to 46 days, and all died from respiratory failure.

The patient who had a surgical biopsy (patient 1) had only been treated with antibiotics before the biopsy (day 9) and died 24 days after the onset of symptoms.

PATHOLOGICAL FINDINGS (TABLE 1)

Histologically, nine of 10 cases showed diffuse alveolar damage (DAD) at different phases of evolution. For the open lung biopsy taken on day 9 (patient 1) and lung tissue from two patients who died shortly after the onset of symptoms (patients 2 and 8), the histology was represented mainly by acute (early exudative) phase DAD, with extensive hyaline membrane formation, a variable degree of alveolar haemorrhage and fibrin in alveolar spaces (Figure 1). The open lung biopsy also showed alveolar space and septal oedema. Coincidental background chronic bronchiolitis was present. Three specimens (patients 6, 9 and 10) taken at 11–21 days showed both acute and organizing (proliferative) phase DAD (Figure 2a). In addition to air space fibrin and hyaline membrane formation, there was septal widening by loose fibroblastic tissue and air space fibromyxoid tissue plugs. Moreover, all showed squamous metaplasia (Figure 2b) of the bronchial epithelium and alveolar lining. Three specimens (patients 4, 5 and 7) taken at 29–46 days were characterized by organizing DAD and fibrosis. In addition to interstitial and air space organization, dense septal and alveolar fibrosis became evident (Figure 3). Features of the acute phase of DAD were no longer seen except for a few remnant hyaline membranes. Features of different phases could be seen in different parts of the same sample. For patient 7, there was, in addition, bronchopneumonia, with abundant neutrophils admixed with fibrin in alveolar spaces (Figure 4).

In the above cases, other variable changes included small to moderate amounts of lymphocytes and foamy macrophages; small amounts of neutrophils; reactive type II pneumocytes characterized by enlarged hyperchromatic nuclei and abundant basophilic cytoplasm; and occasional multinucleated giant cells in alveolar spaces. In patients 8, 9 and 10, there were some enlarged pneumocytes with large nuclei, prominent nucleoli and granular amphophilic cytoplasm. Fibrin thrombi were present in one case (patient 8). None of the cases showed definite viral inclusions. No microorganisms were seen on Gram, Grocott or ZN stain.

One case (patient 3) showed only non-specific inflammatory changes, with focal mild alveolar septal oedema and a mild infiltrate of lymphocytes but no hyaline membrane formation.

Ultrastructural study of lung tissue revealed numerous to moderate numbers of cytoplasmic viral particles in the pneumocytes, many within membrane-bound vesicles. The virus particles were spherical and enveloped, with spike-like projections on the surface and coarse clumps of electron dense material in the centre (Figure 5). Most ranged from 60 to 95 nm in diameter, but occasional ones measured up to 180 nm. In patient 7, there were identifiable bacteria, which was probably the cause for the superimposed bronchopneumonia.

Table 1. Pathological findings and virological data

Case	Sex/ age	Days to death*	Acute-phase DAD	Org. DAD	Fibrosis	Squamous metaplasia	Reactive type II pneumo.	MGC	Pneumo. with cytomegaly	EM on lung tissue	Coronavirus serology		RT-PCR from resp. tract†	RT-PCR from lung‡
											Date	Titre		
1§	M/53	9 (to day of biopsy)¶	+	–	–	+ (in chronic bronchiolitis)	+	–	–	VP	3 March 11 March	1/200 1/1600	+ (NPA)	+
2	F/78	11	+	–	–	–	–	–	–	NA	29 March 3 April	<1/25 1/400	+ (NPA, TS)	+
3	M/31	16	–	–	–	–	–	–	–	VP	NA		+ (NPA)	NA
4	M/45	42	–	+	+	–	+	–	–	NA	22 March 3 April	<1/25 1/200	+ (NPS)	+
5	M/42	29	–	+	+	–	+	–	–	NA	27 March 1 April	<1/25 <1/25	+ (NPA, TA)	–
6	M/67	21	+	+	–	+ (focal)	+	–	–	NA	28 March 3 April	<1/25 1/800	+ (NPA)	–
7	M/50	46	–	+	+	–	+	+ (scanty)	–	VP + bacteria	26 March 27 April	<1/25 1/400	–	NA
8§	F/39	8	+	–	–	–	+ (scanty)	+	+	VP	19 March 22 March	<1/25 1/200	NA	+
9	M/73	20	+	+	–	+ (extensive)	+	+ (scanty)	+	NA	19 March 31 March	<1/25 1/400	+ (NPA)	NA
10	F/40	11	+	+	–	+ (focal)	+	+ (scanty)	+	VP	NA		+ (TS)	+

Org., Organizing; pneumo., pneumocytes; MGC, multinucleated giant cells; NA, not available; VP, viral particles; NPA, nasopharyngeal aspirate; TS, throat swab; NPS, nasopharyngeal swab; TA, tracheal aspirate; RT-PCR, reverse transcription-polymerase chain reaction.

*Days from symptom onset to death.

†RT-PCR for SARS coronavirus from respiratory tract secretion.

‡RT-PCR for SARS coronavirus from lung tissue.

§These two cases have been included in previous reports.[5,6]

¶Patient subsequently died 24 days after symptom onset.

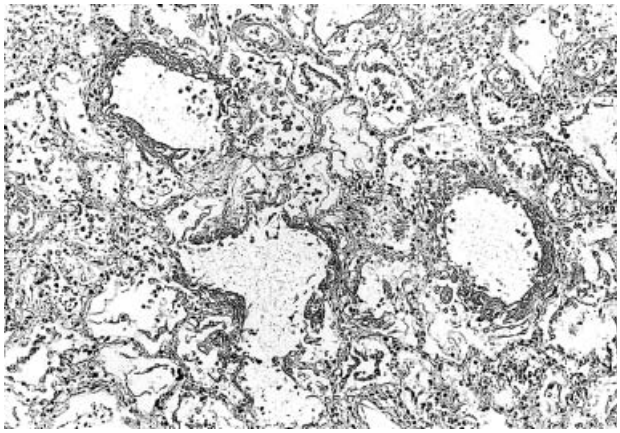

Figure 1. Post mortem lung section from a patient who died on day 8 shows extensive hyaline membrane.

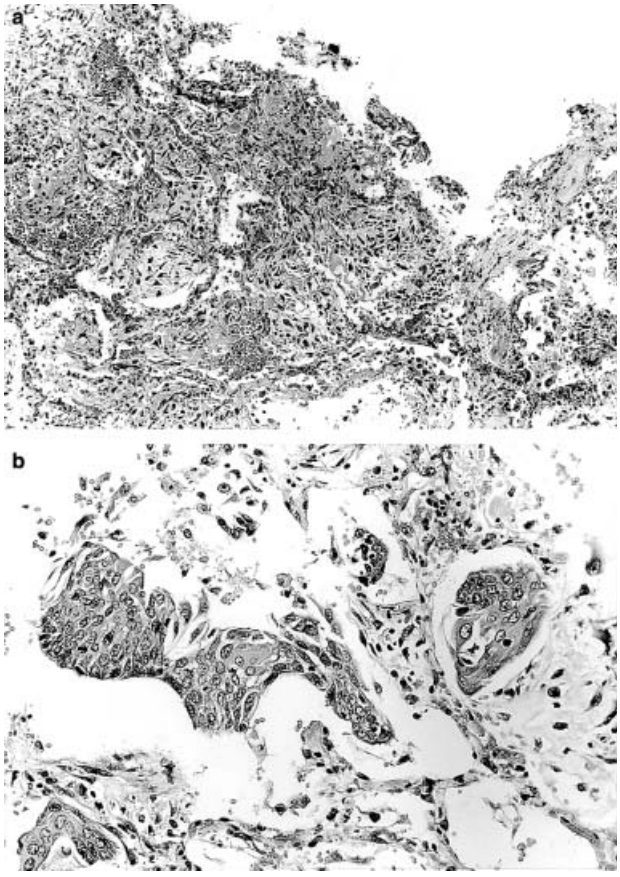

Figure 2. a, Post mortem lung section from a patient who died on day 20 shows air space organization in addition to alveolar fibrin and hyaline membrane. There is also a moderate lymphocytic infiltrate. **b,** Squamous metaplasia is also present.

Discussion

A novel coronavirus (SARS coronavirus) has been shown to be the causative agent of SARS.[1,9]

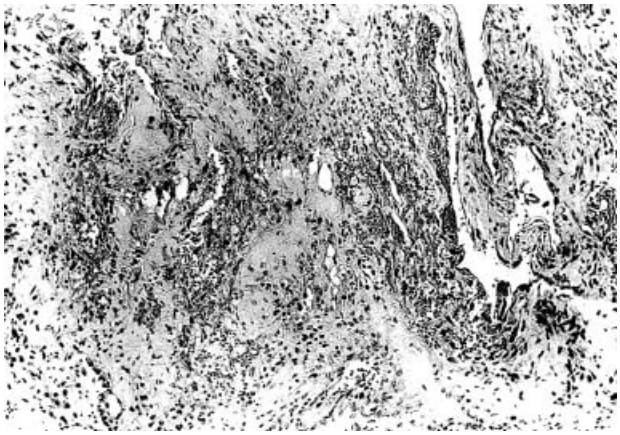

Figure 3. Paramortem lung biopsy from a patient who died on day 46 shows marked fibrosis with distortion of normal alveolar and septal architecture.

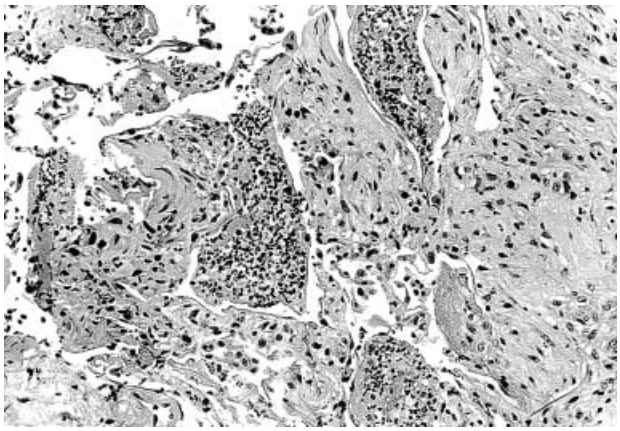

Figure 4. Organizing diffuse alveolar damage with superimposed bronchopneumonia. There are abundant neutrophils in alveolar spaces.

Coronavirus is an RNA virus known to account for up to 30% of common colds in humans and rarely causes lower respiratory tract disease.[10] Instead, it can cause severe respiratory or enteric disease in livestock and poultry.[10] The SARS coronavirus is a new virus affecting the human population and is distantly related to a previously sequenced human coronavirus.[1,9] The virus can be found in respiratory tract secretions, lung tissue, serum and stool.[1,6,11]

The clinical presentation of the SARS patients in this series is similar to those of others.[2,6,12] All presented with fever; other common presenting features are respiratory symptoms and myalgia. While advanced age and presence of pre-existing morbidity have been reported to be associated with adverse outcomes in some series,[2,12] some patients who have succumbed to the disease have been young and otherwise previously healthy.

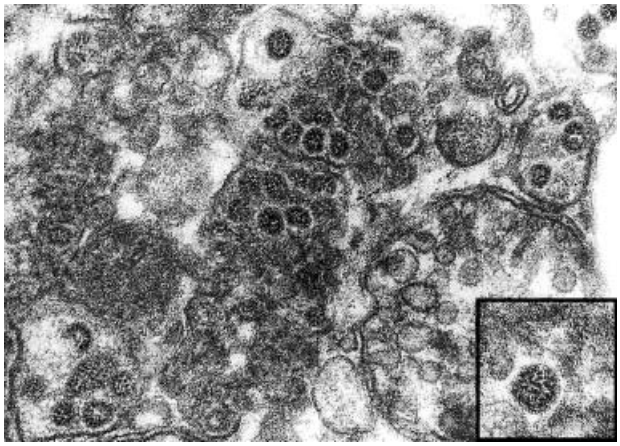

Figure 5. Electron microscopy of the open lung biopsy shows intracytoplasmic viral particles within membrane-bound vesicles (original magnification × 52 000). Inset: A spherical enveloped virion (diameter 88 nm) with spike-like projections on the surface and clumps of electron dense material in the centre (original magnification × 73 000).

With rare exceptions, the main lung pathology in SARS is DAD, which is basically the histological prototype of acute lung injury. The mechanism is believed to be endothelial and alveolar epithelial cell injury leading to fluid and cellular exudation and subsequent reparative fibroblastic proliferation and type II pneumocyte hyperplasia.[13,14] The microscopic appearances depend on the time interval between the insult and biopsy and on the extent of injury.[15] The pathological changes go through discrete but overlapping phases—the early exudative (acute) phase, the proliferative (organizing) phase, and the fibrotic phase.[13,15,16] The process does not necessarily evolve through all stages, and may cease and recover at any stage.[15]

The cases in this series demonstrate the full spectrum of all three phases of DAD, and the features also correspond well with the time sequence of the disease. The specimens taken within 2 weeks after onset of symptoms typically show classical acute-phase DAD, while those taken between the second to third weeks show acute and organizing features. Specimens taken in the fourth week or after show organizing DAD and the fibrotic stage of DAD, a feature which has not been reported in previous series on SARS.[1,2,5–8] Besides the long interval from symptom onset to death, this last group also had the longest duration of mechanical ventilation and the highest concentration of supplementary oxygen of all the patients; thus these factors might also contribute to the late lung damage. So far, no histological material from SARS patients who recover from the disease has been available for comparison; presumably the DAD resolves with or without residual scarring. Similar to previous reports, multinucleated giant cells and cytomegaly of pneumocytes can be observed in some cases.[1,2,5–8] The significance of these cells is not known. Some postulate that the cytomegaly with amphophilic cytoplasm may be a result of viral assembly within the Golgi apparatus.[5] In contrast to a previous report,[5] we did not find foamy macrophages to be the predominant inflammatory cell component, but variable mixtures of lymphocytes, macrophages and neutrophils were found instead. One of the patients in the late stage of DAD showed superimposed pneumonia, and electron microscopic study demonstrated coronavirus as well as bacteria, illustrating the presence of secondary infection which could be a complication of either viral pneumonia or corticosteroid treatment.

The causes of acute lung injury are numerous, and infection and oxygen are among the best documented ones.[15] Among infectious organisms, viruses most consistently produce DAD.[15] Occasionally, fungus, particularly *Pneumocystis carinii*, and bacteria, notably Legionella, can also cause DAD. Measles, adenovirus, herpes virus, cytomegalovirus and influenza virus are well-recognized viruses that can cause acute lung injury, with a diagnostic cytopathic effect noted in the first four.[17–20] Hanta virus has also been reported to cause acute lung injury but shows no specific cytopathic effect.[21,22] The finding of DAD in almost all cases and the persistence of viral particles on electron microscopy even at a late stage (day 46) indicate that SARS coronavirus should be added to the list of causes of acute lung injury manifesting as DAD. The absence of DAD in one patient who had fulfilled all the clinical criteria with positive confirmation test for SARS could be due to a sampling problem, since the paramortem needle biopsy consisted of a few tiny pieces of lung tissue only.

There are apparently no histological features specific for SARS, coronavirus pneumonia, and thus confirmation of the aetiology depends on ultrastructural and virological studies.

Acknowledgement

We thank Dr J. K. C. Chan for his valuable comments on this paper.

References

1. Ksiazek TG, Erdman D, Goldsmith CS *et al.* A novel coronavirus associated with severe acute respiratory syndrome. *N. Engl. J. Med.* 2003; **348;** 1953–1966.

2. Lee N, Hui D, Wu A *et al.* A major outbreak of severe acute respiratory syndrome in Hong Kong. *N. Engl. J. Med.* 2003; **348;** 1986–1994.
3. Cumulative number of reported probable cases of severe acute respiratory syndrome (SARS) (accessed at http://www.who.int/csr/sarscountry/en/). World Health Organization.
4. Hawkey PM, Bhagani S, Gillespie SH. Severe acute respiratory syndrome (SARS): breath-taking progress. *J. Med. Microbiol.* 2003; **52;** 609–613.
5. Nicholls JM, Poon LLM, Lee KC *et al.* Lung pathology of fatal severe acute respiratory syndrome. *Lancet* 2003; **361;** 1773–1778.
6. Peiris JSM, Lai ST, Poon LLM *et al.* Coronavirus as a possible cause of severe acute respiratory syndrome. *Lancet* 2003; **361;** 1319–1325.
7. Franks TJ, Chong PY, Chui P *et al.* Lung pathology of severe acute respiratory syndrome (SARS): a study of 8 autopsy cases from Singapore. *Hum. Pathol.* 2003; **34;** 743–748.
8. Ding Y, Wang H, Shen H *et al.* The clinical pathology of severe acute respiratory syndrome (SARS): a report from China. *J. Pathol.* 2003; **200;** 282–289.
9. Fouchier Ron AM, Kuiken T, Schutten M *et al.* Koch's postulates fulfilled for SARS virus. *Nature* 2003; **423;** 240.
10. Holmes KV. SARS-associated coronavirus. *N. Engl. J. Med.* 2003; **348;** 1948–1951.
11. Drosten C, Gusther S, Preiser W *et al.* Identification of a novel coronavirus in patients with severe acute respiratory syndrome. *N. Engl. J. Med.* 2003; **348;** 1967–1976.
12. Booth CM, Matuka LM, Tomlinson GA *et al.* Clinical features and short-term outcomes of 144 patients with SARS in the Greater Toronto Area. *JAMA* 2003; **289;** 2801–2809.
13. Katzenstein ALA, Bloor CM, Liebow AA. Diffuse alveolar damage—the role of oxygen, shock and related factors. *Am. J. Pathol.* 1996; **85;** 209–228.
14. Bellingan GJ. The pulmonary physician in critical care 6. the pathogenesis of ALI/ARDS. *Thorax* 2002; **57;** 540–546.
15. Katzenstein ALA. Acute lung injury patterns: diffuse alveolar damage and bronchiolitis obliterans—organizing pneumonia. In Katzenstein ALA ed. *Katzenstein and Askin's surgical pathology of non-neoplastic lung disease*, 3rd edn. Philadelphia: W.B. Saunders, 1997; 14–47.
16. Tomashefski JF Jr. Pulmonary pathology of acute respiratory distress syndrome. *Clin. Chest Med.* 2000; **21;** 435–466.
17. Yeldandi AV, Colby TV. Pathologic features of lung biopsy specimens from influenza pneumonia cases. *Hum. Pathol.* 1994; **25;** 47–53.
18. Katzenstein ALA. Infection I. Unusual pneumonias. In Katzenstein ALA ed. *Katzenstein and Askin's surgical pathology of non-neoplastic lung disease*, 3rd edn. Philadelphia: W.B. Saunders, 1997; 247–285.
19. Bencroft DMO. Histopathology of fatal adenovirus infection of the respiratory tract in young children. *J. Clin. Pathol.* 1967; **20;** 561–569.
20. Lheureux P, Verhest A, Vincent JL. Herpes virus infection, an unusual source of adult respiratory distress syndrome. *Eur. J. Respir. Dis.* 1985; **66;** 72–77.
21. Duchin DS, Koster FT, Peters CJ *et al.* Hantavirus pulmonary syndrome: a clinical description of 17 patients with a newly recognized disease. *N. Engl. J. Med.* 1994; **330;** 949–955.
22. Nolte KB, Feddersen RM, Foucar K *et al.* Hantavirus pulmonary syndrome in the United States: a pathological description of a disease caused by a new agent. *Hum. Pathol.* 1995; **26;** 110–120.